Molecular characterization of tumors from a transgenic mouse adrenal tumor model: Comparison with human pheochromocytoma

YOSHIYUKI HATTORI[1], NAOTETSU KANAMOTO[2], KUMI KAWANO[1], HIROSHI IWAKURA[3], MASAKATSU SONE[2], MASAKO MIURA[2], AKIHIRO YASODA[2], NAOHISA TAMURA[2], HIROSHI ARAI[2], TAKASHI AKAMIZU[3], KAZUWA NAKAO[2] and YOSHIE MAITANI[1]

[1]Institute of Medicinal Chemistry, Hoshi University, Shinagawa-ku, Tokyo 142-8501; [2]Department of Medicine and Clinical Science, Kyoto University Graduate School of Medicine, Kyoto 606-8507; [3]Ghrelin Research Project, Translational Research Center, Kyoto University Hospital, Kyoto 606-8507, Japan

Received May 3, 2010; Accepted June 21, 2010

DOI: 10.3892/ijo_00000719

Abstract. Adrenal neuroblastoma and pheochromocytoma have the same embryonic origin from neural crest cells and mainly arise from the adrenal medulla. Recently, transgenic mice exhibiting tumors in the bilateral adrenal medulla by the expression of SV40 T-antigen were developed. In this study, we investigated mRNA expression in adrenal tumors of transgenic mice and compared them with human pheochromocytoma by DNA microarray analysis. To compare mouse adrenal tumors and human pheochromacytoma, we found that the expressions of noradrenergic neuron-related genes, including dopa decarboxylase, phenylethanolamine-N-methyltransferase and chromogranin B, were up-regulated in humans but not in mice; however, the expression of neuroblastoma-related genes, including Mycn, paired-like homeobox 2b, γ-aminobutyric acid A receptor ß3 subunit, islet 1 and kinesin family member 1A, was up-regulated in both species. From the gene expression profiles, the characterization of mouse adrenal tumor, may be similar to that of human adrenal neuroblastoma rather than pheochromacytomas. This mouse model would be a useful tool for the development of anti-cancer drugs and for understanding the etiology of adrenal neuroblastoma.

Introduction

Adrenal neuroblastoma and pheochromocytoma have the same embryonic origin from neural crest cells and mainly arise from the adrenal medulla. Adrenal neuroblastoma is the most common and deadly extracranial solid childhood tumor, exhibiting marked variation in clinical presentation, ranging from localized to high metastatic disease. Neuroblastoma causes 15% of cancer-related deaths in children (1). Patients with early-stage neuroblastoma, particularly those detected by a mass screening program, are known to have a good prognosis, and the tumors of these patients possess the ability to differentiate and regress spontaneously (2). In contrast, patients with advanced-stage neuroblastoma still have a poor prognosis despite recent developments in treatment (1). Pheochromocytomas are catecholamine-producing tumors that occur from chromaffin cells of adrenal medulla or extra-adrenal location, leading to paroxysmal or persistent hyper-tension in most patients (3,4). Pheochromocytoma generally occurs as a benign tumor, but 10-25% of cases are malignant at first surgery or at recurrence, with metastasis development in the lymph nodes, bone, liver or lung. Once pheochromocytoma has metastasized, there is no curative therapy; therefore, the availability of reliable tumor models for adrenal neuroblastoma and pheochromocytoma to test novel chemotherapeutic agents remains an important aspect to improve survival.

For the development of new therapeutic drugs for tumors of the adrenal medulla, *in vivo* rodent models are useful in addition to *in vitro* cultured tumor cells. In the early 1990s, adrenal medullary neoplasms were reported in transgenic mice carrying simian virus 40 (SV40) or polyoma viral T-antigens driven by a variety of promoters (5-8), including those for tyrosine hydroxylase (Th) (8) and phenylethanolamine N-methyltransferase (Pnmt) (6). Some were classified as primitive neuroectodermal tumors (9) or neuroblastoma (5). Better differentiated pheochromocytomas and hyperplastic nodules have subsequently been reported to occur with high frequency in transgenic mice expressing c-mos (10,11) or multiple endocrine neoplasia (MEN) 2B-type mutant rearranged during transfection (RET) (Met 918) (12) and in retinoblastoma (Rb) (13), phosphatase and tensin homolog deleted from chromosome (Pten) (14) or neurofibromatosis 1 (Nf1) (15) knockout mice. Unfortunately, some of these mice have not

Correspondence to: Dr Yoshiyuki Hattori, Institute of Medicinal Chemistry, Hoshi University, Shinagawa-ku, Tokyo 142-8501, Japan
E-mail: yhattori@hoshi.ac.jp

Key words: adrenal tumor, pheochromocytoma, neuroblastoma, DNA array

been maintained and may be permanently lost as experimental models.

Recently, we developed transgenic mice exhibiting tumors in the bilateral adrenal glands by the expression of SV40 T-antigen and have maintained them as a experimental model (16). Genome-wide gene expression studies will provide insight into the genes and molecular pathways that govern the pathogenesis of adrenal tumors; however, this has not been reported in adrenal tumor model mice. In this study, we investigated mRNA expression in adrenal tumors of transgenic mice and compared them with human pheochromocytoma by DNA microarray analysis.

Materials and methods

Animals. Transgenic mice carrying tetracycline inducible SV40 T-antigen, a fusion gene comprising tetracycline-responsive elements (TRE) with cytomegarovirus promoter and SV40 T-antigen were generated by microinjection of fertilized C57/B6 mouse eggs as previously reported (16). Transgenic mice were used as heterozygotes. Animal experiments were conducted with ethics approval from our institutional animal care and use committee.

Histopathology. Excised adrenal tumors from transgenic mice at the age of 5, 9, 13, 15, 17 and 21 weeks (5T, 9T, 13T, 15T, 17T and 21T, respectively) and normal adrenal gland from non-transgenic littermates at the age of 5, 9, 13 and 17 weeks (5N, 9N, 13N and 17N, respectively) were immediately frozen, sectioned 20-μm thick and mounted. The sections were stained with hematoxylin and pure eosin (H&E staining) (Muto Pure Chemicals Co., Ltd., Tokyo, Japan) for histopathological examination.

Tumor procurement. Human tumor specimens were collected from patients who underwent surgery at Kyoto University Hospital (Kyoto, Japan). Specimens were procured under Institutional Review Board-approved protocols compliant with international guidelines and with informed consent from patients. Tumor samples and normal adjacent samples were frozen and stored at -80˚C shortly after surgical resection. Total RNA was extracted from tumors using an RNeasy Midi Kit (Qiagen, Hilden, Germany). The quality and quantity of RNA were sufficient for gene expression profiling in 7 pheochromocytoma and 2 normal adjacent adrenal medulla from 2 patients with pheochromocytoma.

RT-PCR analysis. Total RNA was isolated from mouse adrenal tumors using the RNeasy Midi Kit (Qiagen). RNA yield and purity were checked by spectrometric measurements at 260 and 280 nm, and RNA electrophoresis, respectively. RT-PCR amplification was carried out as previously reported (17). The profile of PCR amplification consisted of denaturation at 94˚C for 0.5 min, primer annealing at 55˚C for 0.5 min, and elongation at 72˚C for 0.5 min for 30 cycles. For the amplification of SV40 T-antigen cDNA, the primers SV40 T-antigen-FW, 5'-AAACACTGCAGGCCAGATTT-3', and SV40 T-antigen-RW, 5'-AAATGAGCCTTGGGACTGTG-3', were used. For the amplification of mouse ß-actin cDNA, the primers ß-actin-FW, 5'-TGTGATGGTGGGAATGGGTCAG-3', and ß-actin-RW, 5'-TTTGATGTCACGCACGATTTCC-3', were used. PCR products were analyzed by 1.5% agarose gel electrophoresis in a Tris-borate-EDTA (TBE) buffer. The products were visualized by ethidium bromide staining.

Real-time RT-PCR was performed on the corresponding cDNA synthesized from each sample described above. The optimized settings were transferred to the real-time PCR protocol with the iCycler MyiQ detection system (Bio-Rad Laboratories, Hercules, CA, USA) and SYBR Green I assay (iQ™ SYBER Green Supermix, Bio-Rad Laboratories) was used for quantification. Samples were run in triplicate and the expression level of each mRNA was normalized for the amount of ß-actin in the same sample. Difference of 1 cycle was calculated as a 2-fold-change in the gene expression.

DNA microarray. For DNA microarray experiments, 0.5 μg aliquots of total RNA from 13N, 13T, 15T, 17T and human tumor specimens were labeled using the Quick Amp Labeling Kit (Agilent Technologies, Santa Clara, CA, USA) according to the manufacturer's instructions. After purification of Cy3-labeled cRNA with RNeasy mini spin columns (Qiagen), 1.65 μg aliquots of Cy3-labeled cRNA were hybridized to Whole Mouse genome Oligo Microarray 44K x 4 (Agilent Technologies) or Whole Human genome Oligo Microarray 44K x 4 (Agilent Technologies) using the manufacturer's hybridization protocol. After the washing step, the microarray slides were analyzed with an Agilent Technologies Microarray scanner.

For further analysis, the data were imported into the GeneSpring® 10 Software (Agilent Technologies) and normalized by median centering of arrays and genes. In mouse adrenal tumors, all transcripts showed a minimum change in the expression level of at least 10-fold compared with the adrenal gland of normal mice. In a comparison of the expression profiles between mouse and human adrenal tumors, hierarchical clustering of the above identified genes in mouse adrenal tumor and image plots using available human orthologues in pheochromocytoma were displayed with gene ordering based on hierarchical clustering of the mouse data set.

Results

Tumor appearance and SV40 T-antigen expression. We previously reported that the ectopic expression of SV40 T-antigen in adrenal medulla developed bilateral adrenal tumors at 12-13 weeks of age in mice (16). In hematoxylin and eosin-stained sections of adrenal glands, mild hyperplasia in the adrenal medulla of transgenic mice was already observed at 5 and 9 weeks of age (Fig. 1A, B, E and F). Subsequently, transgenic mice, beginning at 13 weeks of the age, developed carcinoma of the adrenal gland (Figs. 1I, J and 2A), and by 15 weeks of age, most adrenal tumors were between 0.5 and 1.0 cm in diameter (Fig. 2A). At 17 weeks of the age, tumors of the adrenal glands had enlarged to 1.0-1.5 cm diameter, and at 21 weeks of age, to 1.5-2.0 cm. The tumors in 17T were composed of undifferentiated cells with a large nucleus (Fig. 1M and N) compared with adrenal glands in non-transgenic mice.

Next, we confirmed the expression levels of SV40 T-antigen mRNA in the developing tumors of transgenic mice.

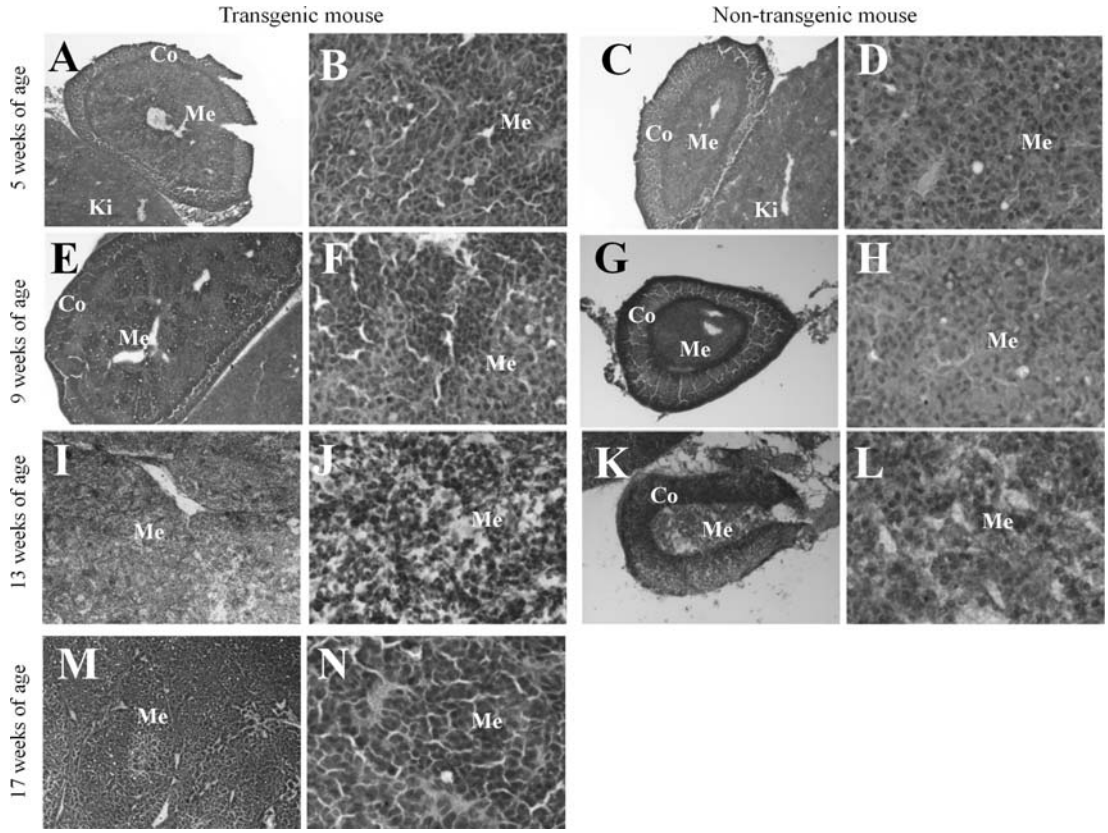

Figure 1. Histological analysis of adrenal gland from transgenic mouse. Histological section of adrenal gland from transgenic mice (A, B, E, F, I, J, M and N) and non-transgenic (C, D, G, H, K and L) mice at 5 weeks (A-D), 9 weeks (E-H), 13 weeks (I-L) and 17 weeks of age (M and N). In B, D, F, H, J, L and N, adrenal medulla in A, C, E, G, I, K and M were enlarged, respectively. H&E staining, x40 in A, C, E, G, I, K and M, x100 in B, D, F, H, J, L and N. Co, cortex of adrenal gland; Me, medulla of adrenal gland; Ki, kidney.

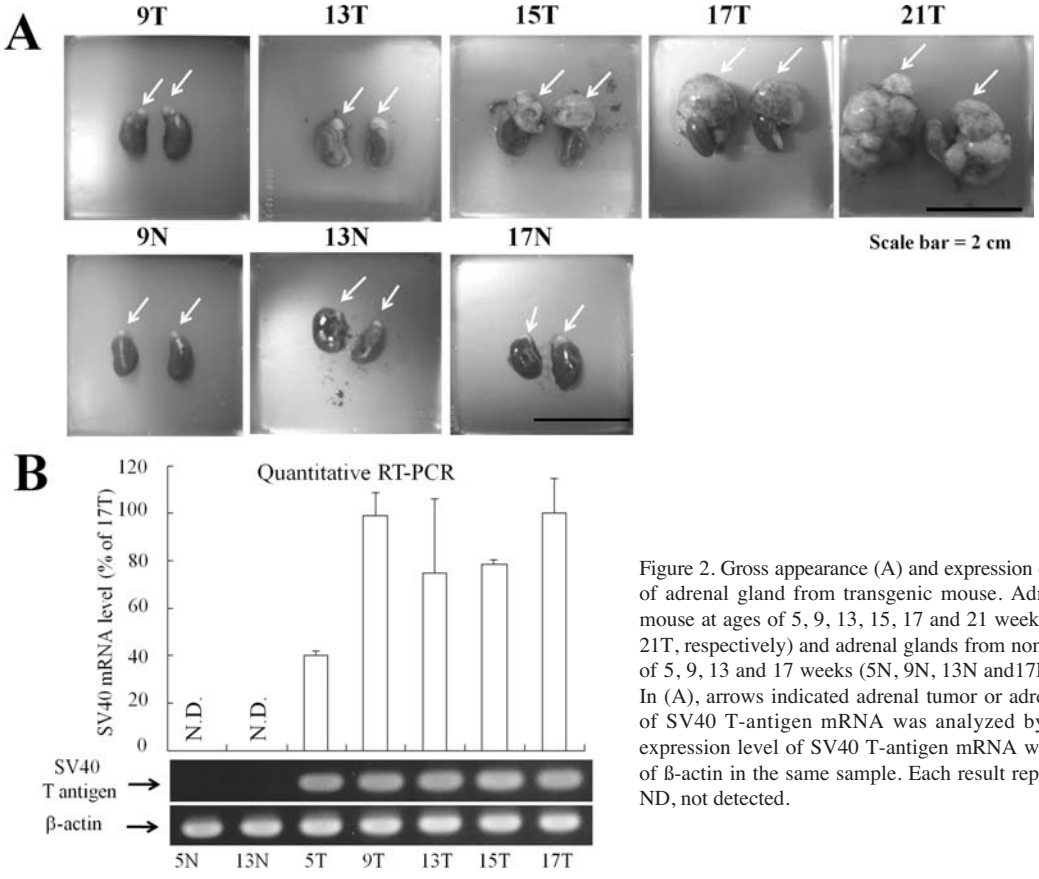

Figure 2. Gross appearance (A) and expression of SV40 T-antigen mRNA (B) of adrenal gland from transgenic mouse. Adrenal tumors from transgenic mouse at ages of 5, 9, 13, 15, 17 and 21 weeks (5T, 9T, 13T, 15T, 17T and 21T, respectively) and adrenal glands from non-transgenic littermates at ages of 5, 9, 13 and 17 weeks (5N, 9N, 13N and17N, respectively) were excised. In (A), arrows indicated adrenal tumor or adrenal gland. In (B), expression of SV40 T-antigen mRNA was analyzed by quantitative RT-PCR. The expression level of SV40 T-antigen mRNA was normalized for the amount of ß-actin in the same sample. Each result represents the mean ± SD (n=3). ND, not detected.

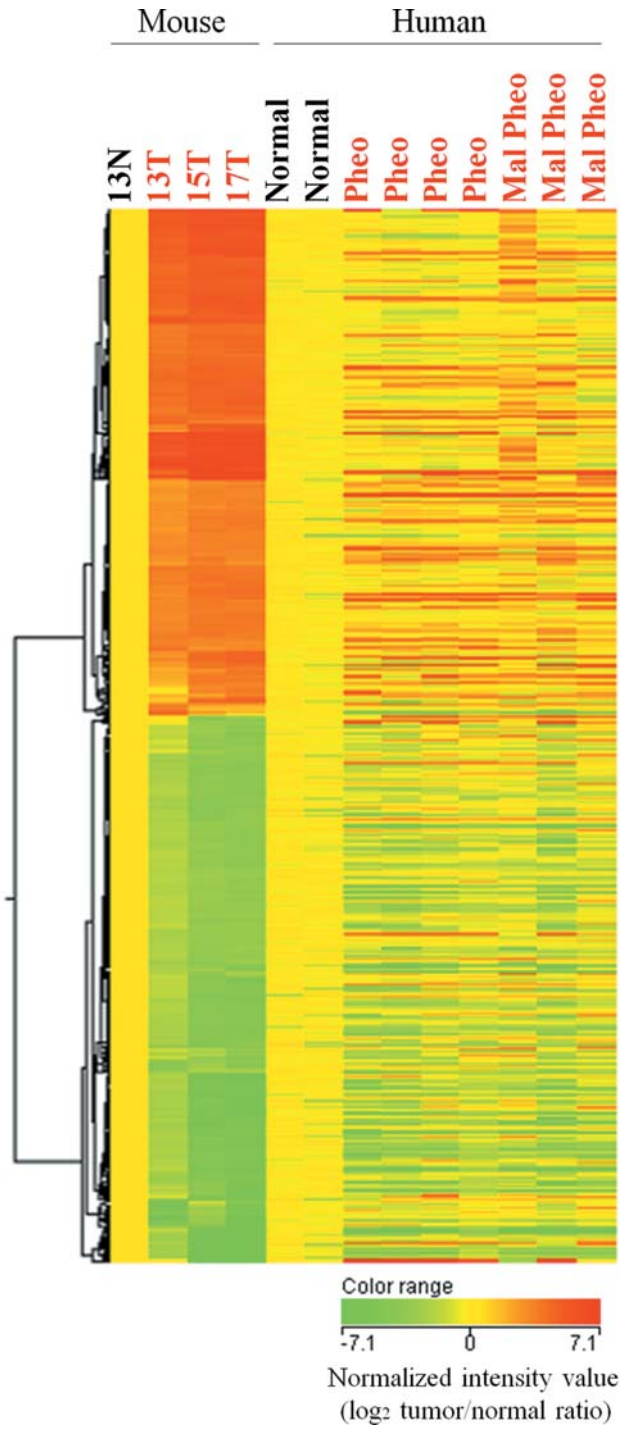

Figure 3. Gene expression patterns of mouse adrenal tumor-specific signature in human pheochromocytoma. Hierarchical clustering of mouse adrenal tumors (13T, 15T and 17T)-specific genes (~2,500 genes), which were >10-fold higher and lower than in the normal adrenal gland (13N), and image plots using available human orthologues in pheochromocytoma are shown with gene ordering based on hierarchical clustering of the mouse data set. Expression profiles in four benign pheochromocytomas (Pheo), three malignant pheochromocytomas (Mal Pheo) and two normal adjacent adrenal medulla (normal) were aligned beside those in mouse tumors. Genes with a relatively higher level of expression are shown in red and those with a lower level of expression in green.

Expression levels of SV40 T-antigen from 5T to 17T were similar, but those in 5N and 13N were not detected (Fig. 2B), suggesting that SV40 T-antigen was expressed in adrenal glands of transgenic mice at an early age and induced adrenal hyperplasia.

Comparison of gene expression patterns between mouse adrenal tumor and human pheochromocytoma. Cells of adrenal neuroblastomas have neuroblastic morphology and do not express the adrenal chromaffin marker Pmnt, but they share phenotypic characteristics with immature sympathetic neuroblasts present as nests of cells in the developing adrenal gland (18). Although sympathetic neurons and chromaffin cells are developmentally related and functionally similar, a defining functional difference between the two cell types is that only chromaffin cells express Pmnt (18).

We compared the expression profile of transgenic mice with that of human pheochromocytoma by DNA microarray (Fig. 3). To investigate mRNA expression in developing adrenal tumors of transgenic mice, we used RNA of adrenal tumors from 13T, 15T and 17T, and of the normal adrenal gland from 13N as a control. Overall, the expression patterns of up- and down-regulated genes in both human benign and malignant pheochromocytomas were similar with those in mouse adrenal tumors (Fig. 3). Furthermore, the expression profile in benign pheochromocytomas was very similar to that in malignant pheochromocytomas, therefore, in subsequent analysis, we used average of four benign and three malignant pheochromocytomas for comparison of expression level with mouse adrenal tumors. In adrenal tumors of transgenic mice, Pmnt expression was absent and other noradrenergic synthesis-related genes also greatly reduced compared with in normal adrenal gland, although up-regulated in human pheochromacytoma (Table I). It has been reported that Pmnt expression was absent or greatly reduced in tumors associated with viral T-antigens (8,19). Furthermore, no difference in blood pressure between transgenic and non-transgenic mice was observed (~60 mmHg in mean blood pressure) (data not shown). These findings indicated that the characteristics of human pheochromocytoma regarding noradrenergic secretion and hypertension were dissimilar to those of mouse adrenal tumors.

Recently, Cheung *et al* have reported that cyclin D1 (CCND1), dopa decarboxylase (DDC), γ-aminobutyric acid A receptor ß3 subunit (GABRB3), islet 1 (ISL1), kinesin family member 1A (KIF1A), and paired-like homeobox 2b (PHOX2B) were abundantly expressed in stage IV human neuroblastoma tumors and these expressions were useful in predicting patient outcome (20). In both mouse and human adrenal tumors, Phox2b, Gabrb3, Isl1 and Kif1a were also up-regulated (Table I). Furthermore, we found 49 up-regulated genes and 66 down-regulated genes which were >10-fold different between a normal adrenal gland and the adrenal tumor in both mice and humans (Tables II and III). Among them, we found that the expressions of doublecortin and CaM kinase-like 1 (Dclk1), dihydropyrimidinase-like 3 (Dpysl3), embryonic lethal, abnormal vision, Drosophila-like 3 (Elavl3), GATA binding protein 2 (Gata2), GATA binding protein 3 (Gata3), hairy/enhancer-of-split related with YRPW motif 1 (Hay1), myelin transcription factor 1-like (Myt1l), transgelin 3 (Tagln3), and transcription factor AP-2 ß (Tcfap2b), which are related to nervous system development, were strongly up-regulated in both human and mouse adrenal tumors (Table II), and the expression of many genes related to lipid metabolic

Table I. Adrenal gland-related genes in human pheochromocytoma and mouse adrenal tumors as shown by cDNA microarray.

Gene symbol	Description	Gene expression (log_2 tumor/normal ratio)				Biological process
		13T/13N	15T/13N	17T/13N	Pheo/ normal	
Noradrenergic neuron-related genes						
Ddc	Dopa decarboxylase	0.64	-3.11	-1.14	7.91	Catecholamine biosynthetic process
Th	Tyrosine hydroxylase	1.06	0.16	-0.30	7.91	Dopamine biosynthetic process from tyrosine
Dbh	Dopamine ß hydroxylase	1.20	1.33	0.89	7.33	Catecholamine metabolic process
Pnmt	Phenylethanolamine-N-methyltransferase	-0.08	-6.33	-8.53	6.10	Catecholamine biosynthetic process
Chga	Chromogranin A	0.17	0.09	-0.18	7.80	
Chgb	Chromogranin B	-0.24	-0.21	-0.06	5.96	
Npy	Neuropeptide Y	-0.08	-0.50	-0.70	7.39	Neuropeptide signaling pathway
Slc6a2	Solute carrier family 6, member 2	2.47	1.25	0.28	7.99	Neurotransmitter transport
Neuroblastoma-related genes						
Phox2b	Paired-like homeobox 2b	1.49	1.86	1.94	9.04	Regulation of transcription
Mycn	V-myc myelocytomatosis viral related oncogene, neuroblastoma derived	0.76	0.97	1.47	5.79	Regulation of progression through cell cycle
Ccnd1	Cyclin D1	-1.97	-3.11	-3.42	0.67	Regulation of progression through cell cycle
Crmp1	Collapsin response mediator protein 1	2.74	3.34	3.27	6.19	
Gabrb3	γ-aminobutyric acid receptor, subunit ß3	2.98	2.82	2.64	4.45	γ-aminobutyric acid signaling pathway
Isl1	ISL1 transcription factor, LIM/homeodomain	4.24	5.99	6.17	4.36	Regulation of transcription
Kif1a	Kinesin family member 1A	0.48	1.50	1.61	6.17	Microtubule-based process

Pheo, human pheochromocytoma; normal, human normal adrenal medulla.

process and electron transport was strongly down-regulated (Table III). The reasons for suppression of the metabolism might be that energy (ATP) in tumor cells is mainly or only provided by glycolysis in the cytoplasm and suppresses oxidative phosphorylation in mitochondria (Warburg effect) (21).

We also found that G protein-regulated inducer of neurite outgrowth 1 (Grin1) (22), insulin-like growth factor 2 gene (Igf2) (23), embryonic lethal, abnormal vision, Drosophila-like 4 (Elavl4) (24), and cadherin-like 22 (Cdh22) (25), which are known to relate with neuroblastoma progression, were strongly up-regulated in both mouse and human adrenal tumors (Table II). These identified genes might be important for the development of adrenal tumors in mice and humans. From gene expression profiles, the characterization of mouse adrenal tumor might be similar to that of human adrenal neuroblastoma rather than pheochromacytoma.

Discussion

In this study, we investigated mRNA expression in adrenal tumors of transgenic mice carrying SV40 T-antigen by DNA microarray analysis. The SV40 T-antigen oncoprotein binds to and functionally inactivates two major tumor suppressor genes, Rb and p53, which are often involved in many human tumors, and strongly affects many genes associated with DNA replication, damage repair, cytokinesis, and chromosome maintenance. It has been reported that proliferative gene expression patterns driven by the SV40 T-antigen were shared by transgenic mice carrying SV40 T-antigen, which

Table II. The highly up-regulated (>10-fold) genes both in human pheochromocytoma and mouse adrenal tumor (17T) as shown by cDNA microarray.

Gene symbol	Description	Gene expression (log_2 tumor/normal ratio)				Biological process
		13T/13N	15T/13N	17T/13N	Pheo/ normal	
A2bp1	Ataxin 2-binding protein 1	3.02	3.72	3.45	3.45	
Abcc8	ATP-binding cassette, sub-family C, member 8	3.54	4.94	4.93	4.64	Carbohydrate metabolic process
Bai3	Brain-specific angiogenesis inhibitor 3	4.23	5.11	5.17	4.23	Signal transduction
Cartpt	CART prepropeptide	6.52	6.56	5.83	6.21	Neuropeptide signaling pathway
Cdh22	Cadherin-like 22	3.06	3.72	3.52	7.70	Cell adhesion
Celsr3	Cadherin, EGF LAG seven-pass G-type receptor 3	3.31	3.54	3.54	5.74	Neuropeptide signaling pathway
Chrm2	Cholinergic receptor, muscarinic 2	-0.29	2.94	3.38	3.45	Signal transduction
Chrna5	Cholinergic receptor, nicotinic, α5	3.55	3.65	3.96	3.46	Signal transduction
Clgn	Calmegin	5.16	6.18	6.40	7.56	Protein folding
Coro2a	Coronin, actin binding protein, 2A	3.22	3.65	3.43	3.95	
Crtac1	Cartilage acidic protein 1	5.25	6.00	5.99	3.79	
Cryba2	Crystallin, ßA2	4.42	4.53	5.02	7.99	
Dclk1	Doublecortin and CaM kinase-like 1	4.57	6.38	6.83	5.93	Nervous system development
Dpysl3	Dihydropyrimidinase-like 3	2.66	4.26	4.64	3.90	Nervous system development
Elavl3	ELAV-like 3	4.48	5.20	5.31	4.01	Nervous system development
Elavl4	ELAV-like 4	5.01	6.07	5.90	6.22	mRNA processing
Elavl4	Elongation of very long chain fatty acids-like 4	5.64	6.05	5.85	3.87	Fatty acid biosynthetic process
Erc2	ELKS/RAB6-interacting/ CAST family member 2	4.07	3.75	3.90	3.89	Synaptogenesis
Flrt1	Fibronectin leucine rich transmembrane protein 1	3.46	3.22	3.56	5.53	
Galnt6	UDP-N-acetyl-α-D-galactosamine: polypeptide N-acetylgalactosaminyl transferase 6	4.21	4.75	4.23	3.78	Protein amino acid O-linked glycosylation
Gata2	GATA binding protein 2	4.27	3.91	4.02	5.50	Neuron differentiation
Gata3	GATA binding protein 3	3.46	3.89	3.87	4.87	Nervous system development
Gpr68	G protein-coupled receptor 68	4.02	4.98	4.53	4.07	Signal transduction
Gprin1	G protein regulated inducer of neurite outgrowth 1	3.43	3.98	3.83	4.38	
Hand1	Heart and neural crest derivatives expressed 1	5.04	4.99	4.70	4.36	Angiogenesis
Hey1	Hairy/enhancer-of-split related with YRPW motif 1	3.43	3.84	4.21	4.79	Nervous system development
Igf2	Insulin-like growth factor 2	3.87	2.60	3.34	3.55	Cell proliferation
Isl1	ISL1 transcription factor, LIM/homeodomain	4.24	5.99	6.17	4.36	Multicellular organismal development

Table II. Continued.

Gene symbol	Description	Gene expression (log_2 tumor/normal ratio)				Biological process
		13T/13N	15T/13N	17T/13N	Pheo/ normal	
Kcnj12	Potassium inwardly-rectifying channel, sub-family J, member 12	3.10	3.86	3.77	3.46	Ion transport
Kif5a	Kinesin family member 5A	3.74	4.45	4.63	3.58	Microtubule-based movement
Kl	Klotho	1.29	3.56	3.75	5.34	Metabolic process
Lingo1	Eucine rich repeat and Ig domain containing 1	6.47	6.63	6.53	4.59	
Lmo1	LIM domain only 1	3.06	4.47	4.23	5.33	Cell proliferation
Mab21l1	Mab-21-like 1	4.67	5.23	5.05	5.14	Anatomical structure morphogenesis
Mgat5b	Mannosyl (α1,6)-glycoprotein ß-1,6-N-acetyl -glucosaminyltransferase	2.49	3.04	3.64	3.53	
Myt1l	Myelin transcription factor 1-like	3.46	3.31	3.41	3.60	Nervous system development
Nefl	Neurofilament, light polypeptide 68 kDa	4.53	6.79	6.94	8.23	
Prph1	Peripherin	4.82	6.05	6.33	7.53	
Rab39b	RAB39B, member RAS oncogene family	3.76	4.52	4.11	4.70	Protein transport
Rimbp2	RIMS binding protein 2	3.65	4.72	4.46	5.66	
Slc10a4	Solute carrier family 10, member 4	2.46	4.01	4.01	6.92	Ion transport
Stac	SH3 and cysteine rich domain	2.13	3.66	3.60	3.74	Intracellular signaling cascade
Stmn4	Stathmin-like 4	5.06	6.03	5.50	5.86	Intracellular signaling cascade
Syt11	Synaptotagmin XI	3.66	4.13	4.25	4.59	Transport
Tagln3	Transgelin 3	2.84	3.74	3.72	7.25	Nervous system development
Tcfap2b	Transcription factor AP-2 ß protein 2	5.06	5.08	5.19	7.75	Nervous system development
Thbs4	Thrombospondin 4	3.36	6.29	6.19	4.07	Cell adhesion
Tm6sf2	Transmembrane 6 superfamily member 2	-0.10	0.93	4.49	3.48	
Tmem145	Transmembrane protein 145	3.19	3.14	3.39	4.25	
Tubb2b	Tubulin, ß 2B	3.35	5.00	4.84	6.90	Microtubule-based movement

Pheo, human pheochromocytoma; normal, human normal adrenal medulla.

developed breast tumor (C3(1)/Tag transgenic mice driven by rat prostate steroid binding protein promoter), lung tumor (CC10-Tag transgenic mice driven by mouse clara cell secretory protein promoter), and prostate tumor (TRAMP transgenic mouse driven by rat probasin promoter) (26). Therefore, we compared the expression profiles of the SV40 T-antigen signature between adrenal tumors and three tumor types of transgenic mice carrying SV40 T-antigen, and the expression profile of mouse adrenal tumor was very similar to other tumor types of transgenic mouse (data not shown).

The SV40 T-antigen gene signature was not a feature of tumors initiated by other oncogenes or inactivation of suppressor genes but is most specific to tumors induced by T-antigen (26). Transgenic overexpression of myc, ras, HER-2/neu, and polyoma viral middle T-antigen (PyMT) oncogenes driven by mouse mammary tumor virus (MMTV) promoter were most dissimilar to those of SV40 T-antigen in gene expression profiles; however, SV40 T-antigen viral oncoprotein can cause an intrinsic gene expression profile that recapitulates the aggressive phenotypes of aggressive

Table III. The highly down-regulated (>10-fold) genes both in human pheochromocytoma and mouse adrenal tumor (17T) as shown by cDNA microarray.

Gene symbol	Description	Gene expression (log_2 tumor/normal ratio)				Biological process
		13T/13N	15T/13N	17T/13N	Pheo/ normal	
Aadac	Arylacetamide deacetylase	-6.00	-3.34	-6.80	-9.25	Metabolic process
Abca8b	ATP-binding cassette, sub-family A, member 8	-1.29	-2.50	-3.94	-3.71	Transport
Abcb1a	ATP-binding cassette, sub-family B, member 1	-2.15	-4.34	-3.98	-3.56	Transport
Abcb4	Homo sapiens ATP-binding cassette, sub-family B, member 4	-2.60	-5.65	-5.95	-3.95	Lipid metabolic process
Ace2	Angiotensin I converting enzyme 2	-1.63	-3.13	-5.97	-4.09	Proteolysis
Adh1	Alcohol dehydrogenase 1C, γ polypeptide	-1.87	-5.69	-7.09	-3.68	Alcohol metabolic process
Adh4	Alcohol dehydrogenase 4, pi polypeptide	-4.96	-2.80	-4.09	-4.33	Alcohol metabolic process
Agtr1a	Angiotensin II receptor, type 1	-2.00	-5.16	-5.90	-3.53	Signal transduction
Alas1	Aminolevulinate, Δ, synthase 1	-2.40	-5.64	-5.98	-4.69	Biosynthetic process
Aldh1l1	Aldehyde dehydrogenase 1 family, member L1	-2.60	-5.11	-5.71	-5.24	Biosynthetic process
Aldob	Aldolase B, fructose-bisphosphate	-5.84	-2.99	-6.61	-3.87	Metabolic process
Aox1	Aldehyde oxidase 1	-2.47	-5.25	-5.28	-7.73	Electron transport
Apoc1	Apolipoprotein C-I	-3.17	-3.52	-5.65	-6.02	Lipid metabolic process
Baiap2l1	BAI1-associated protein 2-like 1	-2.25	-3.82	-3.40	-3.74	
C3	Complement component 3	-3.32	-5.79	-7.26	-3.63	Signal transduction
C4b	Complement component 4B	-2.39	-3.31	-4.23	-5.20	Inflammatory response
Ccbe1	Collagen and calcium binding EGF domains 1	-2.52	-7.10	-8.16	-4.00	Phosphate transport
Cfi	Complement factor I	-5.94	-2.31	-4.75	-4.28	Proteolysis
Cldn1	Claudin 1	-2.01	-4.58	-3.63	-4.55	Cell adhesion
Cp	Ceruloplasmin	-2.31	-3.24	-3.89	-4.40	Ion transport
Cpb1	Carboxypeptidase B1	-2.45	-8.04	-8.28	-7.08	Proteolysis
Cth	Cystathionase	-2.70	-4.11	-4.63	-4.16	Amino acid biosynthetic process
Cyp11a1	Cytochrome P450, family 11 subfamily A, polypeptide 1	-2.37	-6.60	-8.45	-7.31	Lipid metabolic process
Cyp11b2	Cytochrome P450, family 11, subfamily B, polypeptide 2	-2.60	-8.00	-8.52	-10.92	Lipid metabolic process
Cyp21a1	Cytochrome P450, family 21, subfamily A, polypeptide 2	-2.94	-7.98	-8.85	-9.26	Electron transport
Dab2	Disabled homolog 2, mitogen-responsive phosphoprotein	-2.09	-4.78	-4.81	-3.50	Cell proliferation
Ephx1	Epoxide hydrolase 1, microsomal	-2.11	-3.39	-3.50	-5.78	Xenobiotic metabolic process

Table III. Continued.

Gene symbol	Description	Gene expression (log_2 tumor/normal ratio)				Biological process
		13T/13N	15T/13N	17T/13N	Pheo/ normal	
Fbp1	Fructose-1,6-bisphos-phatase 1	-4.55	-3.04	-5.59	-3.58	Carbohydrate metabolic process
Fdx1	Ferredoxin 1,	-1.68	-4.92	-5.41	-5.51	Steroid metabolic process
Fdxr	Ferredoxin reductase	-2.63	-5.59	-5.71	-5.11	Lipid metabolic process
Fgg	Fibrinogen γ chain, transcript variant γA	-5.63	-1.67	-4.92	-3.83	Signal transduction
Fmo2	Flavin containing monooxygenase 2 (non-functional)	-2.09	-4.05	-4.94	-3.48	Electron transport
Fmo3	Flavin containing monooxygenase 3	-4.03	-6.19	-5.74	-3.60	Electron transport
Galm	Galactose mutarotase	-2.84	-3.59	-3.76	-4.61	Carbohydrate metabolic process
Gata6	GATA binding protein 6	-2.36	-4.96	-5.60	-5.41	Positive regulation of transcription
Gckr	Glucokinase regulator	-4.45	-2.80	-3.94	-3.75	Cell glucose homeostasis
Gja1	Gap junction protein, α1, 43 kDa	-2.20	-4.26	-4.26	-4.24	Transport
Gsta3	Glutathione S-transferase A3	-2.30	-4.07	-6.29	-9.05	Metabolic process
Hsd11b1	Hydroxysteroid (11ß) dehydrogenase 1	-2.18	-3.53	-4.40	-3.95	Metabolic process
Hsd3b1	Hydroxy-Δ-5-steroid dehydrogenase, 3ß- and steroid Δ-isomerase 1	-2.70	-6.67	-8.14	-11.81	Steroid biosynthetic process
Inmt	Indolethylamine N-methyltransferase	-3.51	-3.56	-5.86	-3.36	
Kcnk3	Potassium channel, subfamily K, member 3	-2.40	-4.59	-5.16	-3.46	Ion transport
Kcnn2	Potassium intermediate/ small conductance calcium-activated channel, sub-family N, member 2	-1.87	-6.01	-7.75	-4.25	Ion transport
Ly6d	Lymphocyte antigen 6 complex, locus D	-2.35	-7.54	-9.04	-5.49	Cell adhesion
Mc2r	Melanocortin 2 receptor	-2.54	-6.00	-6.44	-5.29	Signal transduction
Mgst1	Microsomal glutathione S-transferase 1	-2.11	-5.55	-6.29	-7.98	Glutathione metabolic process
Mlxipl	MLX interacting protein-like	-1.75	-4.33	-5.82	-5.18	Regulation of transcription
Mrap	Melanocortin 2 receptor accessory protein	-2.60	-7.07	-8.40	-6.05	
Nr0b1	Nuclear receptor subfamily 0, group B, member 1	-2.63	-7.14	-8.16	-9.23	Adrenal gland development
Nr0b2	Nuclear receptor subfamily 0, group B, member 2	-2.89	-4.98	-5.17	-6.43	Cholesterol metabolic process
Nr1h4	Nuclear receptor subfamily 1, group H, member 4	-2.74	-4.58	-6.70	-6.93	Transcription
Nr5a1	Nuclear receptor subfamily 5, group A, member 1	-2.24	-4.95	-5.14	-5.45	Transcription

Table III. Continued.

Gene symbol	Description	Gene expression (log_2 tumor/normal ratio)				Biological process
		13T/13N	15T/13N	17T/13N	Pheo/ normal	
Pdgfra	Platelet-derived growth factor receptor α polypeptide	-2.13	-3.83	-4.69	-4.61	Cell proliferation
Prlr	Prolactin receptor	-2.36	-4.45	-4.63	-3.46	Steroid biosynthetic process
Rgn	Regucalcin	-4.31	-3.35	-6.08	-5.15	
Rnf43	Ring finger protein 43	-2.58	-4.67	-6.19	-4.94	
Scarb1	Scavenger receptor class B, member 1	-2.13	-5.29	-5.83	-5.53	Cholesterol metabolic process
Sec14l4	SEC14-like 4	-2.44	-3.45	-6.50	-3.53	Transport
Slc37a2	Solute carrier family 37, member 2	-2.19	-3.17	-3.77	-4.60	Transport
Soat1	Sterol O-acyltransferase 1	-2.72	-4.95	-5.38	-4.39	Lipid metabolic process
Star	Steroidogenic acute regulator, nuclear gene encoding mitochondrial protein	-1.73	-6.67	-8.63	-8.64	Steroid biosynthetic process
Steap4	STEAP family member 4	-1.68	-2.51	-3.96	-3.50	Electron transport
Tbx3	T-box 3	-1.86	-4.69	-5.22	-4.77	Anti-apoptosis
Tcf21	Transcription factor 21	-2.07	-2.76	-5.20	-3.88	Organ morphogenesis
Tspan12	Tetraspanin 12	-2.09	-4.89	-5.29	-3.49	
Tst	Thiosulfate sulfurtransferase	-2.44	-4.79	-5.00	-4.70	Sulfate transport
Wnt4	Wingless-type MMTV integration site family, member 4	-2.86	-7.27	-7.73	-3.78	Multicellular organismal development

Pheo, human pheochromocytoma; normal, human normal adrenal medulla.

human cancers (26). In hematoxylin and eosin-stained sections, mouse adrenal tumor was composed of undifferentiated cells with a large nucleus (Fig. 1M and N). From comparison of the gene expression profiles by hierarchical clustering, up- or down-regulated genes in mouse adrenal tumor were overall similar to those in human pheochromocytoma (Fig. 3), but the expression patterns of noradrenergic neuron-related genes in mouse adrenal tumor were dissimilar with those in human pheochromocytoma (Table I), indicating that the characterization of mouse adrenal tumor was similar to that of human adrenal neuroblastoma rather than pheochromocytoma. This transgenic mouse might be a useful model of undifferentiated and aggressive adrenal neuroblastoma.

Researchers are studying chemotherapy drugs in order to find an effective therapy for neuroblastoma. In chemotherapy for high-risk neuroblastoma, the following drugs are often used: cyclophosphamide, ifosfamide, cisplatin, carboplatin, vincristine, doxorubicin (DXR), melphalan, etoposide (VP-16), teniposide (VM-26), and topotecan. In this study, we found that the expression of DNA topoisomerase II (Topo IIα) mRNA in adrenal tumors of transgenic mice increased 120-150-fold compared to non-transgenic mice (data not shown); therefore, we investigated the antitumor effect for transgenic mice by DXR, which is an inhibitor of Topo IIα. As a result, i.v. administration of DXR could suppress tumor growth significantly (data not shown), corresponding with the prognostic results from DNA array; therefore, this mouse model would be a useful tool for the development of anti-cancer drugs of neuroblastoma.

Acknowledgements

This study was supported in part by a Grant-in-Aid for Scientific Research from the Ministry of Education, Culture, Sports, Science, and Technology of Japan, and by the Open Research Center Project.

References

1. Brodeur GM, Maris JM, Yamashiro DJ, Hogarty MD and White PS: Biology and genetics of human neuroblastomas. J Pediatr Hematol Oncol 19: 93-101, 1997.
2. Yamamoto K, Hanada R, Kikuchi A, *et al*: Spontaneous regression of localized neuroblastoma detected by mass screening. J Clin Oncol 16: 1265-1269, 1998.
3. Tischler AS: Pheochromocytoma and extra-adrenal paraganglioma: updates. Arch Pathol Lab Med 132: 1272-1284, 2008.
4. Adler JT, Meyer-Rochow GY, Chen H, *et al*: Pheochromocytoma: current approaches and future directions. Oncologist 13: 779-793, 2008.

5. Aguzzi A, Wagner EF, Williams RL and Courtneidge SA: Sympathetic hyperplasia and neuroblastomas in transgenic mice expressing polyoma middle T antigen. New Biol 2: 533-543, 1990.
6. Hammang JP, Baetge EE, Behringer RR, Brinster RL, Palmiter RD and Messing A: Immortalized retinal neurons derived from SV40 T-antigen-induced tumors in transgenic mice. Neuron 4: 775-782, 1990.
7. Helseth A, Siegal GP, Haug E and Bautch VL: Transgenic mice that develop pituitary tumors: a model for Cushing's disease. Am J Pathol 140: 1071-1080, 1992.
8. Suri C, Fung BP, Tischler AS and Chikaraishi DM: Catecholaminergic cell lines from the brain and adrenal glands of tyrosine hydroxylase-SV40 T antigen transgenic mice. J Neurosci 13: 1280-1291, 1993.
9. Fung KM, Chikaraishi DM, Suri C, *et al*: Molecular phenotype of simian virus 40 large T antigen-induced primitive neuroectodermal tumors in four different lines of transgenic mice. Lab Invest 70: 114-124, 1994.
10. Schulz N, Propst F, Rosenberg MM, *et al*: Patterns of neoplasia in c-mos transgenic mice and their relevance to multiple endocrine neoplasia. Henry Ford Hosp Med J 40: 307-311, 1992.
11. Schulz N, Propst F, Rosenberg MP, *et al*: Pheochromocytomas and C-cell thyroid neoplasms in transgenic c-mos mice: a model for the human multiple endocrine neoplasia type 2 syndrome. Cancer Res 52: 450-455, 1992.
12. Smith-Hicks CL, Sizer KC, Powers JF, Tischler AS and Costantini F: C-cell hyperplasia, pheochromocytoma and sympathoadrenal malformation in a mouse model of multiple endocrine neoplasia type 2B. EMBO J 19: 612-622, 2000.
13. Williams BO, Schmitt EM, Remington L, *et al*: Extensive contribution of Rb-deficient cells to adult chimeric mice with limited histopathological consequences. EMBO J 13: 4251-4259, 1994.
14. You MJ, Castrillon DH, Bastian BC, *et al*: Genetic analysis of Pten and Ink4a/Arf interactions in the suppression of tumorigenesis in mice. Proc Natl Acad Sci USA 99: 1455-1460, 2002.
15. Jacks T, Shih TS, Schmitt EM, Bronson RT, Bernards A and Weinberg RA: Tumour predisposition in mice heterozygous for a targeted mutation in Nf1. Nat Genet 7: 353-361, 1994.
16. Iwakura H, Ariyasu H, Kanamoto N, *et al*: Establishment of a novel neuroblastoma mouse model. Int J Oncol 33: 1195-1199, 2008.
17. Hattori Y and Maitani Y: Folate-linked nanoparticle-mediated suicide gene therapy in human prostate cancer and nasopharyngeal cancer with herpes simplex virus thymidine kinase. Cancer Gene Ther 12: 796-809, 2005.
18. Wong DL: Why is the adrenal adrenergic? Endocr Pathol 14: 25-36, 2003.
19. Tischler AS, Freund R, Carroll J, *et al*: Polyoma-induced neoplasms of the mouse adrenal medulla. Characterization of the tumors and establishment of cell lines. Lab Invest 68: 541-549, 1993.
20. Cheung IY, Feng Y, Gerald W and Cheung NK: Exploiting gene expression profiling to identify novel minimal residual disease markers of neuroblastoma. Clin Cancer Res 14: 7020-7027, 2008.
21. Moreno-Sanchez R, Rodriguez-Enriquez S, Marin-Hernandez A and Saavedra E: Energy metabolism in tumor cells. FEBS J 274: 1393-1418, 2007.
22. Nakata H and Kozasa T: Functional characterization of Galphao signaling through G protein-regulated inducer of neurite outgrowth 1. Mol Pharmacol 67: 695-702, 2005.
23. Hedborg F, Ohlsson R, Sandstedt B, Grimelius L, Hoehner JC and Pahlman S: IGF2 expression is a marker for paragaglionic/SIF cell differentiation in neuroblastoma. Am J Pathol 146: 833-847, 1995.
24. Swerts K, De MB, Dhooge C, *et al*: Potential application of ELAVL4 real-time quantitative reverse transcription-PCR for detection of disseminated neuroblastoma cells. Clin Chem 52: 438-445, 2006.
25. Zhou J, Li J, Chen J, Liu Y, Gao W and Ding Y: Over-expression of CDH22 is associated with tumor progression in colorectal cancer. Tumour Biol 30: 130-140, 2009.
26. Deeb KK, Michalowska AM, Yoon CY, *et al*: Identification of an integrated SV40 T/t-antigen cancer signature in aggressive human breast, prostate, and lung carcinomas with poor prognosis. Cancer Res 67: 8065-8080, 2007.